ISTANBUL TECHNICAL UNIVERSITY ★ GRADUATE SCHOOL OF SCIENCE ENGINEERING AND TECHNOLOGY

DYNAMICAL SYSTEMS ANALYSIS IN COSMOLOGY

M.Sc. THESIS

Ezgi CANAY

Department of Physics Engineering

Physics Engineering Programme

JUNE 2018

ISTANBUL TECHNICAL UNIVERSITY ★ GRADUATE SCHOOL OF SCIENCE ENGINEERING AND TECHNOLOGY

DYNAMICAL SYSTEMS ANALYSIS IN COSMOLOGY

M.Sc. THESIS

Ezgi CANAY
(509151108)

Department of Physics Engineering

Physics Engineering Programme

Thesis Advisor: Assoc. Prof. A. Savaş ARAPOĞLU

JUNE 2018

İSTANBUL TEKNİK ÜNİVERSİTESİ ★ FEN BİLİMLERİ ENSTİTÜSÜ

DİNAMİK SİSTEM ANALİZİNİN KOZMOLOJİDEKİ UYGUMALARI

YÜKSEK LİSANS TEZİ

Ezgi CANAY
(509151108)

Fizik Mühendisliği Anabilim Dalı

Fizik Mühendisliği Programı

Tez Danışmanı: Doç. Dr. A. Savaş ARAPOĞLU

HAZİRAN 2018

Ezgi CANAY, a M.Sc. student of ITU Graduate School of Science Engineering and Technology 509151108 successfully defended the thesis entitled "DYNAMICAL SYSTEMS ANALYSIS IN COSMOLOGY", which she prepared after fulfilling the requirements specified in the associated legislations, before the jury whose signatures are below.

Thesis Advisor :	**Assoc. Prof. A. Savaş ARAPOĞLU** Istanbul Technical University	.....
Jury Members :	**Assoc. Prof. A. Savaş ARAPOĞLU** Istanbul Technical University	.....
	Prof. Dr. Neşe ÖZDEMİR Istanbul Technical University	.....
	Prof. Dr. Özgür DELİCE Istanbul Technical University	.....

Date of Submission : **3 May 2018**
Date of Defense : **5 June 2018**

To my family,

FOREWORD

I would like to express my sincere gratitude and appreciation to Assoc. Prof. Dr. A. Savaş Arapoğlu for his guidance, supervision and encouraging attitude over the course of my Masters's studies. I wish to thank İskender Yalçınkaya for his endless support and belief in me and also for his valuable comments on this manuscript that I appreciate on both academic and personal grounds. I would like to thank A. Emrah Yükselci for his collaboration in our research, computational support and very helpful discussions during the preparation of this thesis.

I am most grateful to my mother, for all she has done.

June 2018 Ezgi CANAY

TABLE OF CONTENTS

Page

ABBREVIATIONS

GR	**:** General relativity
FRW	**:** Friedmann - Robertson - Walker
CMB	**:** Cosmic microwave background
CDM	**:** Cold dark matter
WEC	**:** Weak energy condition
ODE	**:** Ordinary differential equations
Mpc	**:** Megaparsec

SYMBOLS

$(-,+,+,+)$	: Metric signature
$G_{\mu\nu}$	: Einstein tensor
κ	: Gravitational coupling constant in four dimensions
$\kappa_{(4+n)}$	: Higher dimensional gravitational coupling constant
M_{pl}	: Planck mass
$T^{\mu}{}_{\nu}$	: Stress-energy tensor
k	: Curvature index
$g_{\mu\nu}$	: Metric tensor
$\Gamma^{\rho}{}_{\mu\nu}$	: Affine connection
$R^{\rho}{}_{\mu\sigma\nu}$	: Riemann tensor
$R_{\mu\nu}$	: Ricci tensor
R	: Ricci scalar
Ω_i	: Dimensionless energy density parameters
∇_{μ}	: Covariant derivative
Λ	: Cosmological constant
η	: Comoving horizon
ω	: Equation of state parameter
R^n	: N-dimensioanl real coordinate space
λ_i	: Eigenvalues of the stability matrix

LIST OF TABLES

Page

LIST OF FIGURES

Page

DYNAMICAL SYSTEMS ANALYSIS IN COSMOLOGY

SUMMARY

High precision observations in cosmology today reveal that the universe is going through an accelerated expansion that may not be attributed to any conventional energy source in the context of general relativity. Moreover, based on evidences like the shapes of galaxy rotation curves and gravitational lensing data, cosmologists claim the existence of some non-baryonic pressureless dark matter which interacts only gravitationally and makes up about 27 % of the universe.

The hot Big Bang scenario gives an account of the evolution up to late-time acceleration; however, needs to be supported by inflation-like theories due to the so-called flatness and horizon problems. The ΛCDM model, as the standard model of Big Bang cosmology, provides a fairly sound theoretical ground for current observations and introduces the cosmological constant as the source of negative pressure ($\omega_\Lambda = -1$) capable of driving acceleration (again, in the context of GR). Physically, the cosmological constant can be attributed to the vacuum energy density of matter fields but sadly, the measured energy density associated with dark energy in the universe ($\rho_\Lambda \approx 10^{-47}\mathrm{GeV}^4$) does not satisfy the theoretically allowed values ($\rho_\Lambda \approx 10^{74}\mathrm{GeV}^4$) on any grounds.

Given the shortcomings of the standard model, cosmologists have been working on alternative approaches that may come in various ways. Some models propose modifications to the matter sector of the field equations whereas others propose theories beyond GR to model the universe. Due to the ever increasing number of available models in the literature, one may wish to test whether they are in agreement with fundamental observations and relevant measurements. A very practical way of evaluation follows from sketching the global behavior of solutions for the target set-ups. Dynamical system analysis of cosmological models, in this sense, is very useful to indicate whether the system will move towards a stable attractor, and if the parameters are chosen properly, the process allows also for comparison with predictions of modern cosmology.

The thesis presents the study of a five dimensional cosmological model by means of dynamical systems approach. Higher dimensional cosmology has long been studied in the context of alternative theories and the idea originates from the initial attempt of unification by Kaluza and Klein that combined the information of electromagnetism and gravity in five dimensional vacuum. Today, brane world scenarios with non-compactified extra dimensions and universal extra dimensions offering dark matter candidates through compactification are the most common versions of higher dimensional applications in cosmology.

The metric is taken as

$$ds^2 = -dt^2 + a^2(t)\left[\frac{dr^2}{1-kr^2} + r^2(d\theta^2 + sin^2\theta\, d\phi^2)\right] + b^2(t)\, dy^2$$

and the resulting field equations are then cast into the autonomous form

$$\Omega_c' = 2\Omega_c\Big[\Omega_c + \omega_5(1+\Omega_c+\Omega_h) + 1\Big]$$
$$\Omega_h' = 1 - \Omega_h^2 + \Omega_c(1+\Omega_h) + (1+\Omega_c+\Omega_h)\Big[(2+\Omega_h)\omega_5 - 3\omega\Big]\,.$$

The evolution of curvature density Ω_c, and that of higher dimensional scale factor in $\Omega_h = {}^{(\dot{b}/b)}\!/_{(\dot{a}/a)}$ are investigated for different combinations of equation of state parameters (ω, ω_5). Due to the constraints on the four dimensional gravitational *constant* that get as tight as $|\dot{\kappa}/\kappa| = 10^{-11}\ yr^{-1}$ and the necessity of recovering four dimensional cosmology in the final picture, only attractors with $\Omega_h = 0$ are favored. The first group of trajectories satisfying this condition require a negatively curved space in three dimensions for the combination $\omega = \omega_5 = 1/4$, and therefore may only be considered for the earlier epochs. The second group does allow for a flat space in stable equilibrium; however, requires $\omega_5 < -1$ and $\omega < -1/3$ and points at some exotic perfect fluid in the universe.

DİNAMİK SİSTEM ANALİZİNİN KOZMOLOJİDEKİ UYGUMALARI

ÖZET

Modern kozmoloji, güncel gözlemlerin de desteklediği üzere evrenin yeterince büyük ölçekte homojen ve izotropik olduğu prensibi üzerine kuruludur. Dört boyutlu uzay-zamanda çalışılan standart modelde fiziksel mesafeler, bu prensiple uyumlu ve aynı zamanda gravitasyonel alanın da bilgisini içeren Freidmann-Robertson-Walker metriği kullanılarak ifade edilir. Bu metrik, evrenin üç boyuttaki dinamiğinin bilgisini zamana bağlı ölçekleme katsayısı $a(t)$ ile vermektedir. Genel görelilik kapsamında söz konusu metrikten yola çıkılarak elde edilen Einstein alan denklemleri, bu ölçekleme katsayısının ve dolayısıyla evrenin geometrisinin zamana bağlı değişiminin ve aslında en temel olarak gravitasyonel alanın kaynağının evrendeki enerji yoğunluğu olduğunu göstermektedir. Evreni meydana getiren birimler, yine kozmolojik prensiple uyumlu olacak şekilde ideal akışkanlar olarak değerlendirilir. Bunun bir sonucu olarak enerji momentum tensörü yalnızca enerji yoğunluklarını ve bunlara karşılık gelen izotropik basınç değerlerini içerir.

Büyük patlamayı takip eden 10^{-34} saniyenin ardından, evrenin enerji yoğunluğu bakımından sırasıyla ışınımın ve maddenin baskın olduğu evrelerden geçtiği düşünülmektedir. Bu evrelerin her ikisi de evrenin genişleme teorisi ile uyum içinde olsa da, evrenin ivmelenerek genişlediği yönündeki güncel gözlemleri ($\ddot{a} > 0$) alan denklemleri çerçevesinde yalnızca varlığı teorik olarak öne sürülmüş negatif basınçlı karanlık enerji açıklayabilmektedir. Astrofiziksel gözlemler günümüzde evrenin enerji yoğunluğu bakımından yaklaşık %70'lik bölümünü oluşturan karanlık enerjinin ΛCDM modelinde tanımlı olan kozmolojik sabite ait barotropik denklemi ($p_\Lambda = -\rho_\Lambda$) sağladığını ortaya koymaktadır. Bu sabitin varlığı her ne kadar ivmelenmeyi açıklasa da, beraberinde teori temelli sorunlar getirir. Gözlemsel olarak enerji yoğunluğu oldukça küçük bir değerle ($|\rho_\Lambda| \approx 10^{-47}$ GeV^4) sınırlıdır ve bu değer, kozmolojik sabitin fiziksel olarak karşılık gelmesi beklenen kuantum alanlarının vakum enerji yoğunluğuyla ($\rho_\Lambda \approx 10^{74}$GeV^4) uyuşmaz.

Gökyüzünü tarayan COBE, WMAP ve PLANCK uydularından elde edilen veriler evrenin 2.7 K sıcaklığında ve $1/10^{-4}$ hassasiyetinde izotropik arka alan ışınımıyla çevrili olduğunu ortaya koymuştur. Sözkonusu ışınımın, büyük patlamayı izleyen $380,000$ yılın sonunda yüksüz atomların oluşması ve ışığın yüklü parçacıklar ile etkileşme mecburiyetinin ortadan kalkması, yani bir nevi *serbest* kalmasıyla bugüne ulaştığı düşünülmektedir; dolayısıyla bu ışınım evrenin o anki görüntüsünü taşır. Kozmik arka alan ışınımının incelenmesiyle elde edilen veriler, günümüzde kozmolojinin standart modeli olarak kabul edilen ve ΛCDM'nin de kaynağı olan büyük patlama senaryosuna ilişkin bir takım problemler olduğunu ortaya koymaktadır. Evrenin üç boyutta neredeyse düz ($\Omega_c = -0.052^{+0.049}_{-0.055}$) geometriye sahip olması ve son saçılma yüzeyinde birbirleriyle haberleşmeleri imkansız görünen noktaların aynı sıcaklıkta olmaları, 1981 yılında Alan Guth tarafından enflasyon teorisinin

ortaya atılmasına yol açmıştır. Daha sonra Linde, Albrecht ve Steinhardt tarafından geliştirilen enflasyon teorisi, büyük patlamayı takip eden $10^{-35} - 10^{-33}$ saniyeleri aralığında evrenin yaklaşık e^{60} kat genişlediğini öne sürmekte ve modern kozmolojide büyük patlamanın tamamlayıcı bir parçası olarak düşünülmektedir.

Günümüzde kozmoloji alanında yapılan çalışmalar, gözlemler ve parçacık fiziğinden gelen deneysel verilerle uyumlu, standart model ve kozmolojik sabitin barındırdığı problemlere çözüm getiren ve kendi içerisinde fiziksel çelişkiler barındırmayan bir evren modeli geliştirme motivasyonunu taşımaktadır. Evrenin erken ve geç evrelerindeki dinamikleri doğru modellemek adına yapılan çalışmalardan bazıları, alan denklemlerinin sağ tarafına enflasyon teorisinde öne sürülen skaler alanlar gibi alternatif enerji kaynakları eklemeyi öngörürken, bir bölümü de kozmik ölçeğin modellenmesinde genel rölativiteye alternatif teorilere yönelmektedir. Bu tez kapsamında beş boyutlu bir evren modeli dinamik sistemler yaklaşımıyla incelenecek ve sonuçların güncel gözlemlerle uyumu tartışılacaktır.

Yüksek boyutlu modellerin temeli, 1920'li yıllarda Kaluza ve Klein tarafından elektromanyetik ve gravitasyonel alanlara ait bilginin beş boyutlu boş uzay-zamanda birleştirilmesiyle atılmıştır. Bunu izleyen dönemlerde, büyük birleşik teori arayışında öne çıkan sicim teorisi ve benzeri çalışmalarda yüksek boyutlar fikri sıkça kullanılmış ve elbette bu fikir kozmolojide de ilgili modellerde yer bulmuştur. Bu türden yaklaşımların kozmolojideki karşılıklarını iki grup altında incelemek mümkün olabilir. Bunlardan ilki, ekstra boyutların saptanamayacak büyüklükte enerji seviyelerine ve dolayısıyla, yine saptanamayacak ölçekteki uzunluklara atfedildiği *evrensel ekstra boyutlar*dır. Bir tür *kompaktlaştırma* süreci içeren ve bunun sonucunda karanlık madde olmaya aday *zayıf etkileşen kütleli parçacıklar* üreten bu modeller, gözlemlerle uyum sağlanabilmesi açısından beraberinde ekstra boyutların erken evrelerde stabilize olması gerekliliğini getirir. On bir boyutta tanımlı olan sicim ve M-kuramlarından gelen zar evrenler modeli ise ekstra boyutların madde alanlarına kapalı olarak tanımlanması sayesinde kompaktifikasyon süreçleri gerektirmez. Bunların yanında, ekstra boyutların dinamiğinden faydalanarak ivmelenmeyi ve karanlık enerjinin doğasını açıklamayı hedefleyen kozmolojik modeller de literatürde mevcuttur.

Alan denklemlerinin işaret ettiği kozmolojik modelleri dinamik sistem analizinden faydalanarak incelemek oldukça pratik bir yaklaşım gibi gözükmektedir. Bunun için, öncelikle anlamlı değişkenler tanımlanır ve dinamik süreçleri modelleyen denklemler otonom diferansiyel denklem seti haline getirilir. Denge durumlarına ait çözümler bulunduktan sonra faz uzayının bu çözümler etrafındaki topolojik yapısını incelemek mümkün olur ve elde edilen yörüngeler sayesinde sistemin global davranışının bilgisine hızlıca ulaşılabilir. Çözümlerin asimptotik olarak varacağı kararlı denge durumu (eğer var ise) tayin edilebilir ve modelin geçerliliği bu bağlamda test edilmiş olur.

Tez kapsamında ele alınan model

$$ds^2 = -dt^2 + a^2(t)\left[\frac{dr^2}{1-kr^2} + r^2(d\theta^2 + sin^2\theta\, d\phi^2)\right] + b^2(t)\, dy^2$$

metriğinden yola çıkılarak kurulmuş ve ardından ilgili alan denklemleri, ekstra boyutun ve uzay eğriliğinin dinamiğini içeren değişkenler cinsinden otonom diferansiyel denklem setine dönüştürülmüştür. Önceden belirtilen adımlar izlenerek kararlı denge çözümlerine giden yörüngeler elde edilmiş ve bunların arasından standart

kozmolojideki verilerle uyum gözetilerek sadece $\dot{b} = 0$ durumunu sağlayan, yani asimptotik olarak stabilize ekstra boyuta gidenler araştırılmıştır. Bu yörüngelerden ilki, yüksek boyutlu ışınım tipindeki izotropik bir enerji kaynağı ($p = \rho/4$), ve daha genel olarak $3\omega + \omega_5 = 1$ ilişkisini sağlayan dört boyutta anizotropik de olabilecek rölativistik kaynaklar için bulunmuştur. Asimptotik olarak $\dot{b} = 0$ durumunu sağlayan çözümler beraberinde negatif eğriliğe sahip bir uzay getirmiş, dolayısıyla model bu kapsamda ancak erken evreni incelemek için anlamlı bulunmuştur. İkinci tip yörüngeler stabilize boyutun yanında düz evren koşulunu da sağlamış, ancak barotropik denklem katsayıları $\omega_5 < -1$ ve $\omega < -1/3$ kısıtlamalarına tabi bulunmuştur.

1. INTRODUCTION

Cosmology is an extensive field of study in physics that aims to reveal the mechanisms governing the dynamics of the universe. Understanding the earlier patterns of its structure, and ultimately, obtaining a complete picture for the entire evolution of the universe requires a careful analysis of its geometry, past and current energy compositions including the dark sector, and a comprehensive study of various theories modeling interactions that may have occurred earlier at energy scales yet unreachable at the ground-based accelerators. The hot Big Bang model developed in this sense stands as the backbone of most cosmological studies today and is also referred to as the standard model of cosmology in the literature. The ΛCDM model, with its roots in the Big Bang theory, matches the high-precision observations to a very good extent, but at the same time, inspires many other theories in search of alternatives for Λ-attributed late-time acceleration and the very mysterious early characteristics of the universe.

1.1 Fundamental Observations in Modern Cosmology

As first realized by Edwin Hubble in 1929, galaxies recede away from each other at speeds proportional to the respective distances in between. The linear relation obeys [2, 3]

$$v = Hd\,, \tag{1.1}$$

where H is referred to as the *Hubble constant*.

Consistently, current observational evidence coming from *standard candles* like type Ia supernovae adds up to the fact that the universe is expanding. Moreover, deviations from Hubble law indicate that it is, in fact, *accelerating* [4–8].

Neglecting peculiar velocities of astrophysical objects, distances in cosmology may, therefore, be represented in terms of the *comoving distance* x and the time dependent *scale factor* a(t) such that [9]

$$d = a(t)x\,, \tag{1.2}$$

where, with reference to equation 1.1, $H(t) \equiv \dot{a}/a$.

Examining the large scale structure of the universe [10–12], one also realizes that the distribution of matter over scales of the order of few Mpc has a uniform pattern. Namely, clusters and superclusters of galaxies appear to be positioned evenly over the space. The same information comes from the cosmic background radiation [1, 13, 14] that reaches the observer from when the universe was about 380,000 years old. Big Bang cosmology assumes a hot and dense early universe that has gone through radiation and matter dominated epochs as it cooled and expanded in a decelerating ($\ddot{a} < 0$) manner. An important moment within the history of cosmic evolution is that of *decoupling* at which neutral atoms were formed and radiation was set free to propagate without scattering from free electrons. It appears to the observer in the late-times as the highly isotropic CMB that carries the information of the *last scattering surface* that follows the period of matter-radiation equality. The relic radiation is of remarkably uniform temperature [15]

$$T_0 = 2.7255 \pm 0.0006K \tag{1.3}$$

emphasizing *homogeneity* and *isotropy* also in the early universe. The tiny fluctuations of one part in 10^4 are those of density in the young universe, which are considered to be the origin of structure formation driven later by gravitational attraction. Shapes of galaxy rotation curves are expected to obey Kepler's law that indicates $v \propto r^{-1/2}$ i.e., rotational velocity should decrease with r^2; however, astrophysical observations reveal that moving away from the visible mass, velocity vs. radius curve for galaxies abnormally increases or at least, remains flat [16]. Gravitational lensing effects, associated with bending of photon trajectories due to mass distributions, again imply that there must be some non-visible matter in the universe interacting solely by gravitational means. Gravitational potential responsible for structure formation and CMB anisotropies also supports the argument and the energy denisty of *dark matter* from PLANCK data [1] greatly exceeds that of visible matter as can be seen in Table (1.1).

1.2 General Relativity as the Tool for Cosmology

High precision observations bring the question of which theory fits the data best, and Einstein's theory of general relativity appears as a perfectly convenient framework for

working on the large-scale dynamics of the universe. Revealing the relation between energy and gravity in the remarkably simple and elegant form

$$G_{\mu\nu} = \kappa T_{\mu\nu}\,, \tag{1.4}$$

it allows to express the energy constituents of the universe in terms of their effects on the structure of the curved space-time and relevantly, dynamical size of the spatial sector.

1.2.1 Gravity

In cosmology, the four dimensional Einstein tensor $G_{\mu\nu}$ arises generically from the maximally spatially symmetric Friedmann-Robertson-Walker metric

$$ds^2 = -dt^2 + a^2(t)\left[\frac{dr^2}{1-kr^2} + r^2(d\theta^2 + sin^2\theta d\phi^2)\right] \tag{1.5}$$

or, equivalently,

$$g_{\mu\nu} = \begin{pmatrix} -1 & 0 & 0 & 0 \\ 0 & \frac{a^2(t)}{1-kr^2} & 0 & 0 \\ 0 & 0 & a^2(t)r^2 & 0 \\ 0 & 0 & 0 & a^2(t)r^2 sin^2\theta \end{pmatrix} \tag{1.6}$$

for equation 1.5 may also be expressed as

$$ds^2 = g_{\mu\nu} dx^\mu dx^\nu\,. \tag{1.7}$$

Not surprisingly, the above choice follows from the *cosmological principle* i.e., from the fact that the universe appears homogeneous and isotropic as one extends the scope of his observations up to a few hundred Mpc in space.

The theory of general relativity requires that the effects of gravity be embedded in the geometry of space-time, or more precisely, in the metric $g_{\mu\nu}$ and its derivatives. The LHS of equation 1.4, namely the gravitational sector of the field equations reads [17, 18]

$$G_{\mu\nu} = R_{\mu\nu} - \frac{1}{2} R g_{\mu\nu} \tag{1.8}$$

where $R_{\mu\nu}$ and R are the Ricci (curvature) tensor and the Ricci scalar, respectively. Defining first the tensor-like affine connection as

$$\Gamma^\rho{}_{\mu\nu} \equiv \frac{1}{2} g^{\rho\gamma}(\partial_\mu g_{\nu\gamma} + \partial_\nu g_{\mu\gamma} - \partial_\gamma g_{\mu\nu})\,, \tag{1.9}$$

one may obtain the Riemann tensor

$$R^{\rho}{}_{\mu\sigma\nu} \equiv \partial_{\sigma}\Gamma^{\rho}{}_{\mu\nu} - \partial_{\nu}\Gamma^{\rho}{}_{\mu\sigma} + \Gamma^{\gamma}{}_{\mu\nu}\Gamma^{\rho}{}_{\sigma\gamma} - \Gamma^{\gamma}{}_{\mu\sigma}\Gamma^{\rho}{}_{\nu\gamma} \tag{1.10}$$

which is, indeed, the measure of intrinsic curvature responsible for geodesic deviations on a manifold. Applying $\sigma \to \rho$ to equation 1.10, contraction with the upper index yields the rank-two Ricci tensor

$$R^{\rho}{}_{\mu\rho\nu} = R_{\mu\nu}\,, \tag{1.11}$$

and making use of the inverse metric $g^{\mu\nu}$, the Ricci scalar can then be derived through

$$R_{\mu\nu}g^{\mu\nu} = R\,. \tag{1.12}$$

1.2.2 Energy-momentum tensor

Matter in the universe is regarded as a *perfect fluid* for which the energy-momentum tensor $T^{\mu}{}_{\nu}$ takes the form

$$T^{\mu}{}_{\nu} = (\rho + p)u^{\mu}u_{\nu} + p\delta^{\mu}_{\nu} \tag{1.13}$$

with ρ as the matter energy density and p, the isotropic pressure. The four velocity $u^{\mu} = dx^{\mu}/d\tau$ is regarded as that of the observer in a frame comoving with the fluid so that $u^{\mu} = (-1,0,0,0)$ and eventually,

$$T^{\mu}{}_{\nu} = \begin{pmatrix} -\rho & 0 & 0 & 0 \\ 0 & p & 0 & 0 \\ 0 & 0 & p & 0 \\ 0 & 0 & 0 & p \end{pmatrix}. \tag{1.14}$$

The above tensor above carries the contribution of all forms of energy except gravity [19] and the basic requirement of the conservation of total energy-momentum in the universe translates into the continuity equation as

$$\nabla_{\mu}T^{\mu}{}_{\nu} = 0\,. \tag{1.15}$$

It is assumed that energy density and pressure are related to each other in the simplest case via the barotropic equation of state

$$p = \omega\rho\,, \tag{1.16}$$

in which the constant ω factor, called the Equation of State parameter, helps distinguish between different types of energy forms in the universe. For non-relativistic matter, the relation yields $p_m = 0$ and for radiation, one gets $p_r = \rho_r/3$.

In the absence of interactions, equation 1.15 applies to dust and radiation separately, giving

$$\begin{aligned} \dot{\rho}_m + 3H\rho_m &= 0\,, \\ \dot{\rho}_r + 4H\rho_r &= 0\,. \end{aligned} \tag{1.17}$$

1.3 A Glimpse at the Late-Time Behavior

Given the maximally spatially symmetric FRW metric and the energy momentum tensor with vanishing off-diagonal elements, the only independent equations following from the field equations in 1.4 appear as

$$3H^2 + 3\frac{k}{a^2} = \kappa\rho \tag{1.18}$$

coming from $G_{00} = \kappa T_{00}$ and

$$2\dot{H} + 3H^2 + \frac{k}{a^2} = -\kappa p \tag{1.19}$$

from the spatial elements $G_{ij} = \kappa T_{ij}$.

For practical purposes that will appear clear in the following sections, the Friedmann equation in 1.18 may also be expressed in terms of the dimensionless energy density parameters Ω_i and Ω_c, so that it reads

$$1 + \Omega_c = \sum_i \Omega_i \tag{1.20}$$

where $\Omega_c = k/a^2H^2$ and $\Omega_i = \kappa\rho_i/3H^2$.

The ongoing accelerated ($\ddot{a} > 0$) expansion of the universe in the late-time bears the necessity of going beyond the standard model on theoretical grounds. From equations 1.18 and 1.19, it appears evident that such behavior requires some unconventional energy source with negative pressure. Otherwise, one should turn to modified versions of GR or as well, alternative theories for modeling the late-time behavior.

Moving on with the option of assuming some dark energy component (of unknown origin), the associated energy density parameter announced by the Planck collaboration reads [1]

$$\Omega_{\Lambda,0} = 0.692 \pm 0.012 \tag{1.21}$$

(68% CL, from PLANCK TT+lowP+lensing) to reveal that it makes up about 70% of the total density as it uniformly fills the universe and all the regions otherwise empty of matter [19] .

Table 1.1 : Cosmological parameters from recent Planck data [1].

Parameters	TT+low P+lensing	Parameters	Constraints
$\Omega_b h^2$	0.02226 ± 0.00023		
$\Omega_{DM} h^2$	0.1186 ± 0.0020	Ω_c	$-0.052^{+0.049}_{-0.055}$
$\Omega_m h^2$	0.1415 ± 0.0019		
Ω_m	0.308 ± 0.012		
Ω_Λ	0.692 ± 0.012	ω	$-1.006^{+0.085}_{-0.091}$
H_0	67.81 ± 0.092		

Back in the field equations, equation 1.19 produces deceleration for matter ($\omega_m = 0$) and radiation ($\omega_r = 1/3$) components from WEC i.e., $T_{\mu\nu}u^\mu u^\nu \geq 0$. In attempt to meet the observational constraints, one rewrites the field equations in the form

$$G_{\mu\nu} + g_{\mu\nu}\Lambda = \kappa T_{\mu\nu} \tag{1.22}$$

in which Λ denotes the cosmological constant capable of providing negative pressure with $\omega_\Lambda = -1$. Proposed initially by Perlmutter et al. [20] and Riess et al. [4], it is probably the strongest dark energy candidate as the observations today yield [1]

$$\omega = -1.006^{+0.085}_{-0.091} \tag{1.23}$$

(from PLANCK TT+lensing+ext) in a spatially flat universe.

The particle physics counterpart of cosmological constant is the vacuum energy density and the reason for the *cosmological constant problem* lies exactly in this explanation. The current value of Λ is deduced from the Hubble constant H_0 and the associated energy density reads

$$\rho_\Lambda = \frac{\Lambda}{\kappa} \approx 10^{-47} GeV^4\,, \tag{1.24}$$

whereas the vacuum energy density calculated for quantum fields with mass m yields [21]

$$\rho_{vac} = \int_0^\infty \frac{d^3k}{(2\pi)^3}\sqrt{k^2+m^2}\,. \tag{1.25}$$

For $k_{max} = m_{pl}$, the finite numerical value of the above integral turns out to be $\rho_{vac} \approx 10^{74} GeV^4$.

The huge inconsistency in the orders of magnitude of ρ_Λ and ρ_{vac} makes room for many alternative approaches in modern cosmology ranging from quintessence (canonical scalar field) models to modified gravity theories (see [21] and references therein), all with the purpose of justifying the late-time acceleration.

1.4 Inflation

Big Bang cosmology does not come without its problems. The *comoving horizon* in standard cosmology is a particular measure of distance that defines a constraint for the causally connected regions in the universe. It corresponds to the maximum distance light may travel within some cosmic time t as in

$$\eta \equiv \int_0^t \frac{dt'}{a(t')} = \int_0^a d(lna)\left(\frac{1}{aH}\right). \tag{1.26}$$

The *comoving Hubble radius* $(aH)^{-1}$ may also be expressed in the form [22]

$$(aH)^{-1} = H_0^{-1} a^{\frac{1}{2}(1+3\omega)}, \tag{1.27}$$

which appears to be monotonically growing for $(1+3\omega) > 0$, and therefore, is an indicator of increase in the fraction of the universe that is in causal contact over time. The highly isotropic CMB radiation reaching the observer from the last scattering surface ($a_{ls} \sim 0.001$) presents a puzzling case because the patches that could not have been in causal contact back at a_{ls} exhibit uniform temperature up to $O(10^{-4})$. This is called the *horizon problem*.

The second issue, referred to as the *flatness problem*, is associated with the fine-tuning of initial conditions. Setting $\tilde{\Omega} = \sum_i \Omega_i$ in equation 1.20, one immediately sees that in order to produce a flat space in the generic setup, the total energy density in the universe must be equal to some critical density defined as $\rho_{cr} = 3H^2/\kappa$, so that $\tilde{\Omega} - 1 = 0$. Currently, the numerical value of the Ω_c parameter, as indicated in table 1.1, is very close to zero and equivalently, $\tilde{\Omega}$ diverges from unity by a very small amount. During the matter dominated and radiation dominated epochs, $(aH)^{-1}$ increases to cause deviations from flatness, therefore the values observed today may only be reached if $\tilde{\Omega}$ was much closer to unity, i.e. subject to extreme fine-tuning at earlier epochs as in the conditions below [22]

$$|\tilde{\Omega}(a_{pl}) - 1| \leq O(10^{-61}), \tag{1.28}$$

$$|\tilde{\Omega}(a_{BBN)} - 1| \leq O(10^{-16}). \tag{1.29}$$

The theory of inflation, as a solution to the above mentioned problems, was proposed initially by Guth [23] in 1981 and assumed a period of exponential expansion in the

early universe. Later by Linde [24], and Albrecht and Steinhardt [25], it was revised and became foundation of many models offering mechanisms capable of producing such rapid expansion ($\geq$ 60 e-folds between $t_i = 10^{-35}$s and $t_f = 10^{-33}$s after the Big Bang) in the early universe. A delicate point in the theory is that the accelerated expansion must be brought to an end to allow for a radiation dominated epoch through the *reheating* process.

Homogeneous scalar fields are the most prevalent mechanisms that may drive the accelerated expansion of the universe and therefore, are studied extensively in the context of both early and late-time dynamics.

2. DYNAMICAL SYSTEMS

In the vast field of physics, it is very common to encounter systems subject to time evolution, in which the set of variables describing the problem move from one state to another as part of a dynamical process. In order to see the overall pattern, or technically speaking, the asymptotic behavior in such systems, one usually makes use of methods from the theory of dynamical systems for practical purposes. Given the possibility of treating the universe in such context, this chapter is intended to provide the most basic information on the theory along with means of its proper implementation in cosmology.

2.1 Methods and General Concepts in Dynamical Analysis

Dynamical systems are expressed mathematically in the form of differential (or as well, difference) equations. Written in autonomous from, as they will be throughout this work, these equations reveal at first the *steady states* i.e., equilibrium solutions accessible to the system under analysis. Topological structure of the *phase space* around stationary points then yield the trajectories of existent *solution curves*, so that once the desired initial conditions are set, one may easily trace the behavior of the system at any moment in terms of the associated variables.

The rest of this section covers the step-by-step implementation of the above mentioned process as means of dynamical analysis with an exemplary application to ΛCDM model.

2.1.1 Determination of fixed points and linearization

In the simplest case, nonlinear systems of autonomous ODE's or identically, vector fields have the form [26]

$$\dot{x} = f(x), \tag{2.1}$$

with $x \in U \subset R^n$ and $f : U \to U$ where U is an open subset in R^n. The overdot represents the first order time derivatives of the dependent variables with $t \in R^1$.

A fixed point of equation 2.1 satisfies

$$f(x_0) = 0 \tag{2.2}$$

due to the vanishing tangent vector at $x = x_0$.

In order to properly analyze the time evolution of a dynamical system, it is crucial to define the appropriate phase space accommodating each accessible state that is physically relevant to the given configuration. A phase space — excluding the more general cases — may be as large as the entire R^n or as well, be subject to constraints depending on the choice of variables and of course, their physical interpretations.

Considering the difficulties in solving systems of the form equation 2.1, one usually seeks instead to reveal their local behavior near equilibrium points via topological analysis [27]. For $x = (x_1, x_2, ..., x_n)$ and $f(x) = (f_1(x), f_2(x)...., f_n(x))$, the Taylor expansion about an equilibrium point yields

$$f_i(x_1, x_2, ..., x_n) \approx \sum_{j=1}^{n} \frac{\partial f_i}{\partial x_j}\Big|_{x_j = x_{j0}} (x_j - x_{j0}) \tag{2.3}$$

and the $n \times n$ stability matrix (Jacobian) of the system follows as

$$Df = \frac{\partial f_i}{\partial x_j} = \begin{pmatrix} \frac{\partial f_1}{\partial x_1} & \cdots & \frac{\partial f_1}{\partial x_n} \\ \vdots & \ddots & \vdots \\ \frac{\partial f_n}{\partial x_1} & \cdots & \frac{\partial f_n}{\partial x_n} \end{pmatrix} . \tag{2.4}$$

Calculating the eigenvalues of the stability matrix at $x = x_0$, one may obtain all the necessary information for classifying the topology of the neighboring vector fields.

Parallel to the generic terminology, an *unstable node* or *source* refers to a fixed point that repels all the nearby trajectories. At such points, the Jacobian produces eigenvalues of the form $\lambda_i = \{\alpha_i + i\beta_i : \ \alpha_i > 0, \alpha_i, \beta_i \in R\}$. In two dimensional systems, existence of non-zero imaginary parts, i.e. eigenvalues with $\beta_i \neq 0$ turns the trajectories into *unstable spirals*. The opposite case, with $\lambda_i = \{\alpha_i + i\beta_i : \ \alpha_i < 0, \alpha_i, \beta_i \in R\}$ applies to *stable nodes* or *sinks* that attract the neighboring solution curves. Again, non-zero imaginary parts in the eigenvalues creates spirals in two dimensions, only this time of stable character. Topological sinks possess the characteristics of *asymptotically stable points* such that any nearby solution $y(t)$ obeys

$$\lim_{t \to \infty} y(t) = x_0 \, . \tag{2.5}$$

The third category of equilibrium solutions, *saddles*, entail the existence of eigenvalues with both positive and negative real parts.

A common property of the above defined fixed points is that they are all associated with eigenvalues including non-zero real parts. Such points, in a more general context, are categorized as *hyperbolic fixed points* for which, the local characteristics of the non-linear system in equation.2.1 appears topologically equivalent to that of its linear part.

An equilibrium solution may as well be of *non-hyperbolic* type entailing at least one zero eigenvalue. For the special case of $\lambda_i = \{\alpha_i + i\beta_i \colon \alpha_i = 0, \beta_i \in R \setminus \{0\}\}$, the point becomes a center. While investigating the stability properties of non-hyperbolic points, one refers in general to rather extensive techniques discussed thoroughly in textbooks on dynamical systems and chaos [26–28].

2.1.2 Bifurcations

In some systems, the autonomous equations contain additional control parameters that may affect the stability properties of fixed points. Such systems appear in the form [27]

$$\dot{x} = f(x, \mu) \tag{2.6}$$

that differs from the definition in equation 2.1 only by the additional argument $\mu \in R^m$. Assuming a one-dimensional system for which $\mu \in R^1$, the set of conditions [27]

$$f(x_0, \mu_0) = 0 \tag{2.7}$$

$$\frac{\partial f}{\partial x}(0,0) = 0 \tag{2.8}$$

reveal x_0 as a non-hyperbolic fixed point and $\mu = \mu_0$, as a *bifurcation value* for the system. In higher dimensions,i.e $x \in R^n$ and $\mu \in R^m$, the second condition translates into the requirement that the Jacobian $Df(x_0, \mu_0)$ have at least one zero eigenvalue.

The simplest bifurcations of equilibra are categorized as saddle-node, transcritical, pitchfork and Hopf-type bifurcations, the properties of which are covered extensively in [28]. Exchange of stability properties is associated with transcritical bifurcation which may be studied on the sample one dimesional system

$$\dot{x} = \mu x - x^2 \,. \tag{2.9}$$

According to conditions in 2.7 and 2.8, $\mu = 0$ is a bifurcation value for the above equation. The fixed point located at $x = 0$ is independent of μ; however, the second one at $x = \mu$ does depend on the control parameter and thus, its stability characteristics are expected to differ for $\mu > 0$ and $\mu < 0$.

The very interesting case of Hopf-type bifurcations occur when $Df(x_0, \mu_0)$ yields a pair of purely imaginary eigenvalues whereas the remainder necessarily obeys $\lambda_i = \{\alpha_i + i\beta_i : \alpha_i \in R \setminus \{0\}, \beta_i \in R\}$. If the eigenvalues of the Jacobian cross the imaginary axis at $\mu = \mu_0$, one obtains periodic orbits.

2.2 Cosmology Through Dynamical System Analysis

Dynamical systems approach to cosmology may easiest be demonstrated on ΛCDM model (as in [29, 30]) with matter and radiation components on the RHS of equation 1.22. Since the gravitational sector is built upon the usual FRW metric in Eq. (1.5), field equations read

$$3H^2 = \kappa(\rho_m + \rho_r) + \Lambda\,, \tag{2.10}$$

$$2\dot{H} + 3H^2 = -\tfrac{\kappa}{3}\rho_r + \Lambda \tag{2.11}$$

where the curvature parameter is set to $k = 0$ and as usual, the first relation may be cast into the form

$$1 = \Omega_m + \Omega_r + \Omega_\Lambda\,. \tag{2.12}$$

In attempt to track the evolution of energy densities in such setup, it appears convenient to set the dimensionless parameters on the RHS as the variables in the associated dynamical system.

Using equations 2.10 and 2.11 together with the fluid equations of the form 1.17 for non-interacting matter and radiation components, one obtains [29]

$$\begin{aligned} \Omega_m' &= \Omega_m(3\Omega_m + 4\Omega_r - 3)\,, \\ \Omega_r' &= \Omega_r(3\Omega_m + 4\Omega_r - 4) \end{aligned} \tag{2.13}$$

where prime denotes differentiation with respect to $N = \log a$. The autonomous set above does not include a third equation for Ω_Λ because the constraint in equation 2.12 essentially reduces the system to a two-dimensional problem.

Physically, the energy density parameters of matter and radiation are confined to the intervals $0 \leq \Omega_i \leq 1$ from WEC and additionally, the definition of cosmological

Table 2.1 : Critical points of the autonomous set in equation 2.13 with their eigenvalue dependent stability properties

#	Ω_m	Ω_r	Eigenvalues	Character
A	0	1	$\lambda_1 = 1, \lambda_2 = 4$	Unstable node
B	0	0	$\lambda_1 = -4, \lambda_2 = -3$	Stable node
C	1	0	$\lambda_1 = -1, \lambda_2 = 3$	Saddle node

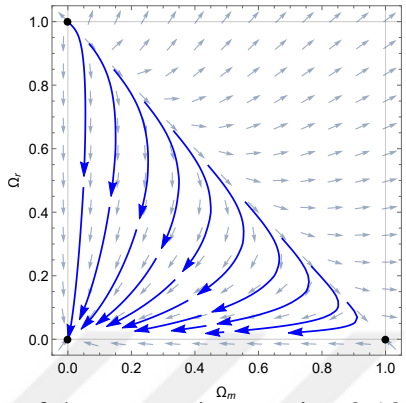

Figure 2.1 : Phase portrait of the system in equation 2.13 under the constraint 2.12.

constant that suggests $\Lambda > 1$. The phase space for the system, then, reduces to the triangular plane in figure 2.1.

Obtaining the fixed points via equation 2.2 and analyzing their stability characteristics by linear approximation (see table 2.1), one may sketch the phase portrait in figure 2.1, in which the corresponding trajectories are illustrated by blue curves on the triangular domain. All the solutions in the phase plane set out from a radiation dominated universe and eventually reach a cosmological constant-dominated state as $n \to \infty$, which is in perfect agreement with the ΛCDM model regardless of the initial conditions. In order to include a matter dominated epoch along the natural evolution of the universe, the trajectories close to the $\Omega_r = 1 - \Omega_m$ line must be favored over others. Considering the very small numerical value of the cosmological constant today, the trajectories of this type reveal the observed evolution pattern to a very good extent.

.

3. FIVE DIMENSIONAL COSMOLOGY

It has long been considered possible in cosmology that the universe may consist of more than the perceivable four dimensions demonstrated in the form of three spatial coordinates and time. Within the framework of general relativity, relevant studies go back to Kaluza-Klein theory (see [31] for a review) that was developed in 1920's as an attempt to unify gravity and electromagnetism in five dimensional empty universe [32]. It served, at the time, as a milestone along the development of unified theories for bringing into the picture the highly appreciated notion of compactification that imposed constraints on the topology of the extra dimension(s) and required the size of the fifth (extra) dimension(s) to remain at non-observable scales [33]. Embracing the idea of higher dimensional unification, the succeeding theories have had their respective impacts on cosmological studies [34–49] where the possible existence of (4+d) dimensions became subject to various interpretations.

Brane world scenarios [50–54], with their roots in string/M theory, propose the existence of a higher dimensional space-time (bulk) in which the propagation of standard model particles is only allowed through the three spatial dimensions (brane). The constraints on the particle propagation here are not only aimed to recover the fundamental observations but also considered to endorse the viability of non-compactified extra dimensions. On the opposite corner, the model of universal extra dimensions [55] allow SM particle propagation through all dimensions and suggest that the generic Kaluze-Klein dimensional reduction would yield Light Kaluz-Klein Particles as strong dark matter candidates in the form of weakly interacting massive particles (WIMPs). Evidently, this approach incorporates the necessity of compactification and stabilization of extra dimensions as would be enforced by the functioning of fundamental interactions. Additionally, the *dynamical reduction* process is also available in alternative interpretations in the literature [35, 36, 56] as the essence of the accelerated expansion of the universe.

3.1 The Need for Stabilization

The observable universe consists of four dimensions, hence in a viable $3+1+n$ dimensional scenario, one should eventually be able to recover the current cosmological structure regardless of the initial set-up.

The four dimensional relation

$$1+\Omega_c = \Omega_{\tilde{\rho}}\,, \tag{3.1}$$

with now $\Omega_{\tilde{\rho}}$ as the energy density parameter of the perfect fluid, can be derived from the FRW metric of the homogeneous and isotropic space through $G_{\alpha\beta} = \kappa T_{\alpha\beta}$ where $\alpha,\beta = 0,1,2,3$ and $\kappa = {}^{8\pi}/_{M^2{}_{pl}}$. In a higher dimensional theory, Planck mass as a fundamental scale relates to its four dimensional counterpart through [52]

$$M^2{}_{pl(4)} = V_{(n)} M^2{}_{pl(4+n)} \tag{3.2}$$

where $V(n)$, the extra-dimensional volume, appears as a time-dependent variable consistent also with the dynamical reduction processes mentioned earlier. Straightforwardly, equation 3.2 translates into

$$\kappa = \frac{\kappa_{(4+n)}}{V_{(n)}}\,, \tag{3.3}$$

and due the dynamically varying size of V(n), the four dimensional gravitational coupling *constant*, i.e. the effective strength of gravity obeys the relation [57]

$$\frac{\dot{\kappa}}{\kappa} = -n\frac{\dot{b}}{b} \tag{3.4}$$

in which, $b(t)$ appears as the extra-dimensional scale factor as in **A.12**. Given the observational and experimental constraints on the time-variation of the gravitational constant [58], one may estimate a rough upper bound for equation3.4 as $|\dot{\kappa}/\kappa| < 10^{-11} yr^{-1}$. Considering the difficulties of constructing a model in which the expansion/contraction rate of extra dimensions is subject to such tight limit, models built upon dynamical reduction require that extra dimensions be stabilized i.e., $\dot{b} = \ddot{b} = 0$ before the Big Bang nucleosynthesis.

In order to ensure consistency with observations, it is also important to recover the standard form of field equations that produce the time evolution of three dimensional energy density. Again, static extra dimensions translate into vanishing $\dot{b}$ and $\ddot{b}$ terms

in the higher dimensional field equations (see **A.12**) that, in this case, safely reduce to equations 1.18 and 1.19 for

$$\rho^{(3)} = V_{(n)}\rho\,. \tag{3.5}$$

3.2 Dynamical Analysis of a Toy Model

In the presence of a single extra dimension in space, the metric of the consequent 5D space-time could be chosen as

$$ds^2 = -dt^2 + a^2(t)\left[\frac{dr^2}{1-kr^2} + r^2(d\theta^2 + sin^2\theta\, d\phi^2)\right] + b^2(t)\, dy^2 \tag{3.6}$$

where y denotes the additional space-like coordinate and b(t), the corresponding scale factor. The field equations then read

$$G_{AB} = \kappa_5 T_{AB} \tag{3.7}$$

with κ_5 as the five dimensional gravitational coupling constant and T_{AB}, the energy-momentum tensor of the higher dimensional perfect fluid. Noted that $A, B = 0, 1, 2, 3, 5$; the non vanishing diagonal elements in

$$T^A{}_B = diag(-\rho, p, p, p, p_5) \tag{3.8}$$

once again confirm that isotropy is preserved in the conventional three spatial dimensions along which pressure is defined identically as $p = \omega\rho$. The EoS parameter along the newly introduced coordinate may be allowed to differ from ω in the most general case to yield $p_5 = \omega_5\rho$. Parallel to the steps in section 1.2.1 with

$$R_{AB} = \partial_C \Gamma^C{}_{AB} - \partial_B \Gamma^C{}_{AC} + \Gamma^C{}_{AB}\Gamma^D{}_{CD} - \Gamma^C{}_{AD}\Gamma^D{}_{BC} \tag{3.9}$$

as the five dimensional expression for the Riemann tensor now, non-zero Christoffel symbols (see **A.2**-**A.6**) yield

$$\begin{aligned} R_{00} &= -\left[3\frac{\ddot{a}}{a} + \frac{\ddot{b}}{b}\right] \\ R_{ij} &= g_{ij}\left[\frac{\ddot{a}}{a} + 2\frac{\dot{a}^2}{a^2} + \frac{\dot{a}}{a}\frac{\dot{b}}{b} + \frac{2k}{a^2}\right] \end{aligned} \tag{3.10}$$

together with the additional element (see **A.7**)

$$R_{55} = b^2\left[\frac{\ddot{b}}{b} + 3\frac{\dot{b}}{b}\frac{\dot{a}}{a}\right]. \tag{3.11}$$

Contraction of equations 3.10 and 3.11 with the inverse metric tensor g^{AB} gives the Ricci scalar as

$$R = 6\left(\frac{\ddot{a}}{a}\right) + 2\frac{\ddot{b}}{b} + 6\left(\frac{\dot{a}}{a}\right)^2 + 6\left(\frac{\dot{a}}{a}\right)\left(\frac{\dot{b}}{b}\right) + 6\frac{k}{a^2} \tag{3.12}$$

and the non-zero components of the field equations take the form (**A.9**-**A.15**)

$$\begin{aligned} 3H^2 + 3Hh + 3\frac{k}{a^2} &= \kappa_5\rho \\ -2\dot{H} - 3H^2 - 2Hh - \dot{h} - h^2 - \frac{k}{a^2} &= \kappa_5(\omega\rho) \\ -3\dot{H} - 6H^2 - 3\frac{k}{a^2} &= \kappa_5(\omega_5\rho) \end{aligned} \tag{3.13}$$

where $\dot{a}/a \equiv H$ stands for the Hubble parameter of the observed space and $\dot{b}/b \equiv h$, for that of the extra dimension.

As mentioned earlier, most studies in extra dimensional cosmology require that stabilization of newly introduced dimensions take place before the Big Bang Nucleosynthesis. In attempt to test the toy model described in equation 3.13 in that sense, one should best trace the behavior of $h(t)$ in the field equations. Applying dynamical system analysis with proper choice of variables helps see, without demanding any exact solutions, whether it is possible to lose the $h(t)$ term along the natural evolution of the universe.

To begin with, the first expression in equation 3.13 may be cast into the form

$$1 + \Omega_h + \Omega_c = \Omega_\rho \tag{3.14}$$

where the dimensionless cosmological parameters are defined as

$$\Omega_\rho = \frac{\kappa_5\rho}{3H^2}\,, \qquad \Omega_h = \frac{h}{H}\,, \qquad \Omega_c = \frac{k}{a^2H^2}\,. \tag{3.15}$$

Calculating their derivatives with respect to $N = \log a$ and making proper substitutions via field equations in equations 3.13 (see **A.22**-**A.26**), one obtains the autonomous equations

$$\begin{aligned} \Omega_\rho' &= \Omega_\rho\Big[(1-3\omega) + 2\omega_5\,\Omega_\rho - (1+\omega_5)\Omega_h\Big]\,, \\ \Omega_h' &= 1 - \Omega_h^2 + \Omega_c + (2\omega_5 - 3\omega)\Omega_\rho + \omega_5\,\Omega_\rho\,\Omega_h + \Omega_c\,\Omega_h\,, \\ \Omega_c' &= 2\Omega_c\Big[\Omega_c + \omega_5\,\Omega_\rho + 1\Big] \end{aligned} \tag{3.16}$$

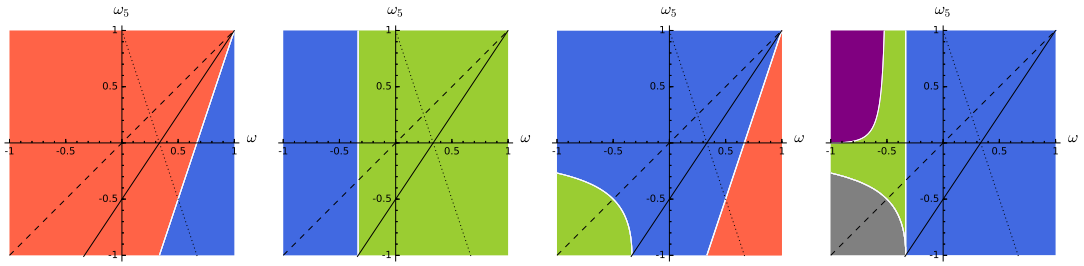

Figure 3.1 : Stability properties of the fixed points with respects to EoS parameters, from left to right: Point A, Point B, Point C and Point D. Red: Unstable node, Blue: Saddle, Green: Stable node, Gray: Saddle for $\Omega_c \geq 0$, Purple: Stable spiral. White curves indicate bifurcations. Three solution categories are shown in lines for combinations $\omega = \omega_5$ (dashed), $3\omega + \omega_5 = 1$ (dotted), $1 + 2\omega_5 - 3\omega = 0$ (straight).

to be used in the dynamical analysis. As a final step in the set-up, it is convenient to reduce the number of independent variables and eliminate Ω_ρ to track explicitly the time evolution of Ω_c and Ω_h instead, where the latter is of prior interest for carrying the information of the extra dimensional scale factor. The autonomous set now takes the form

$$\begin{aligned} \Omega_c' &= 2\Omega_c \Big[\Omega_c + \omega_5(1+\Omega_c+\Omega_h)+1\Big], \\ \Omega_h' &= 1-\Omega_h^2+\Omega_c(1+\Omega_h)+(1+\Omega_c+\Omega_h)\Big[(2+\Omega_h)\omega_5-3\omega\Big] \end{aligned} \tag{3.17}$$

and governs alone the dynamics of the newly introduced cosmological model.

3.2.1 Stability analysis of the fixed points

The two dimensional system defined in 3.17 has four critical points listed in table 3.1. The stability properties they may possess depend explicitly on the control parameters ω and ω_5.

Point A represents a flat universe and a state at which the fifth dimension contracts at a rate equal to that of three dimensional expansion, i.e., $(\Omega_c, \Omega_h) = (0, -1)$. The state appears in [42] in one of the Kasner-type solutions (K1) to a similar set of differential equations, with $H(t)$ and $h(t)$ as the variables which are related to each other via the ansatz $h(t) = c_i H(t)$. The constant c_i described in the mentioned work obeys $c_1 = -1$ for a five dimensional flat universe in the corresponding solution and safely coincides with $\Omega_h = -1$ at Point A.

The curves obeying $\omega_5 = 3\omega - 2$ on the $\omega - \omega_5$ planes in figure 3.1 indicate an interchange of stability between points A and C. The former, therefore, can either

be an unstable node (repeller) or a saddle node on the phase plane depending on the nature of the perfect fluid.

Point B corresponds to a negatively curved (open) universe where the extra dimension appears stabilized with $(\Omega_c, \Omega_h) = (-1, 0)$. For $\omega > -1/3$ the state comes forth as the attractor of the system, and in order to instead obtain a flat universe in the final picture, it becomes inevitable to impose the opposite constraint $\omega < -1/3$.

Point C, like Point A, represents a "flat universe state" over the entire $\omega - \omega_5$ plane. Exact stabilization line $2\omega_5 - 3\omega + 1 = 0$ that is defined to achieve $\Omega_h = 0$ at this point never crosses the attractor zone within $-1 \leq \omega, \omega_5 \leq 1$. Along the line the point exhibits solely saddle properties unless one allows for $\omega_5 < -1$ and $\omega < -1/3$ simultaneously. At $(\omega, \omega_5) = (-1/3, -1)$, it crosses the bifurctaion curve with Point D and thereafter, Point C as an attractor finally allows for stabilization in a flat universe as in figure 3.1. The above mentioned stabilization condition coming directly from dynamical analysis in this case appears in [37] while solving higher dimensional field equations for $a(t)$ and $\rho(t)$ for static ($\dot{b} = 0$) extra dimensions. The second -and last- Kasner-type solution (K3) obtained in [42] for $n = 1$ also makes use of the expression $2\omega_5 - 3\omega + 1 = 0$ while solving again for the Hubble parameters $H(t)$ and $h(t)$ in a set-up identical to 3.13.

There exists two possible bifurcations at Point C; one with Point D across the curve $\omega_5(\omega_5 - 3\omega + 1) + 1 = 0$ and the other with Point A across $\omega_5 = 3\omega - 2$.

Point D, though physically irrelevant to the analysis, is also very rich in bifurcations as can be seen from table 3.1 where both eigenvalues are found to be fully dependent on Eos parameters ω and ω_5. In addition to the previously explored ones, the system manifests Hopf-type bifurcation at this point where periodic solutions arise as the associated eigenvalues cross the imaginary axis.

Mathematically, the point is allowed to exhibit attractor properties for certain combinations of EoS parameters. Physically, however, such states appear to be of no interest because the attractor of the system in equation 3.13 is expected to satisfy $\Omega_h = 0$, and at Point D, the corresponding states lie on the bifurcation line $\omega = -1/3$ (seen in figure 3.1) and *not* within the zone where the point acts as an attractor.

Table 3.1 : Critical points of the autonomous set in 3.17 with their EoS parameter dependent stability properties.

#	Ω_c	Ω_h	Eigenvalues	Condition	Character
A	0	-1	$\lambda_1 = 2$	$\omega_5 > 3\omega - 2$	Unstable node
			$\lambda_2 = \omega_5 - 3\omega + 2$	$\omega_5 < 3\omega - 2$	Saddle node
B	-1	0	$\lambda_1 = -2$	$\omega > -1/3$	Stable node
			$\lambda_2 = -3\omega - 1$	$\omega < -1/3$	Saddle node
C	0	$\frac{2\omega_5 - 3\omega + 1}{1-\omega_5}$	$\lambda_1 = \frac{2\omega_5(\omega_5 - 3\omega + 1) + 2}{1-\omega_5}$	$\lambda_1 > 0 \wedge \lambda_2 > 0$	Unstable node
				$\lambda_1 \cdot \lambda_2 < 0$	Saddle node
			$\lambda_2 = -\omega_5 + 3\omega - 2$	$\lambda_1 < 0 \wedge \lambda_2 < 0$	Stable node
D	$-\frac{\omega_5(\omega_5 - 3\omega + 1) + 1}{(\omega_5 + 1)^2}$	$-\frac{3\omega + 1}{\omega_5 + 1}$	$\lambda_1 = g(\omega, \omega_5) - \sqrt{f(\omega, \omega_5)}$	$g^1 < 0 \wedge f^2 < 0$	Stable spiral
				$\lambda_1 < 0 \wedge \lambda_2 < 0 \wedge f \geq 0$	Stable node
			$\lambda_2 = g(\omega, \omega_5) + \sqrt{f(\omega, \omega_5)}$	$\lambda_1 \cdot \lambda_2 < 0 \wedge f \geq 0$	Saddle node
				$g > 0 \wedge f < 0$	Unstable spiral

[1] $g(\omega, \omega_5) = \frac{3\omega - 2\omega_5 - 1}{2(\omega_5 + 1)}$

[2] $f(\omega, \omega_5) = \frac{3\left[4(\omega_5)^2(2\omega+1) - 4\omega_5(6\omega^2 + \omega - 1) + 3(\omega+1)^2\right]}{4(\omega_5+1)^2}$

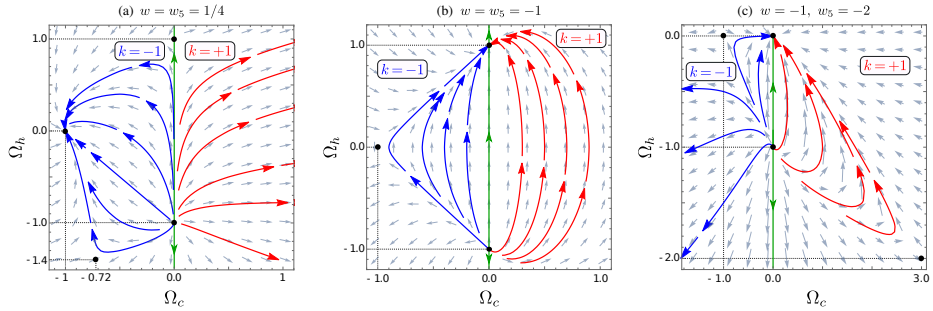

Figure 3.2 : Phase portraits of the system in 3.17 for three sample sets of EoS parameters. Green lines represent solutions in a flat universe. In all diagrams, solution curves below the line $\Omega_h + \Omega_c = -1$ are forbidden to ensure $\Omega_\rho \geq 0$.

3.2.2 Cosmologically viable solutions

Once all the steady states available to the system are located on the phase plane and their accessible stability characters are determined, it becomes possible to distinguish the physically viable scenarios among the resulting trajectories.

Table 3.2 presents a list of cosmologically interesting solutions that include the cases of isotropic (higher dimensional) perfect fluid, stabilization of extra dimension and highly relativistic fluid with the relation $\omega_5 + 3\omega = 1$ in five dimensions.

3.2.2.1 Non-zero curvature

The most interesting solutions appearing in the toy model are, of course, the ones that allow the stabilization of the fifth dimension. The blue trajectories in the left panel of figure 3.2 set a sample for solutions of this kind as they reach $\Omega_h = 0$ (Point B) asymptotically in an open universe model with $k = -1$. The specific example of $\omega = \omega_5 = 1/4$ here corresponds to fully isotropic space filled with highly relativistic fluid only. The EoS parameters associated with such higher dimensional fluid are bound by the relation [37]

$$3\omega + \omega_5 = 1 \tag{3.18}$$

that intersects the line $\omega = \omega_5$ for the combination in question.

In the light of current observations, the $(\Omega_c, \Omega_h) = (-1, 0)$ state as an asymptotic solution may only be allowed during the pre-inflationary epoch because it produces negative curvature against stabilization. Simulating the case with a highly relativistic fluid, then appears to be an appropriate choice for the period of interest is not expected

to allow for energy in non-relativistic form. One must be careful in analyzing the solution categories here, because as shown in the middle panel of figure 3.2, an isotropic fluid in general will not satisfy the stabilization condition; however, an unisotropic one will always do the work as long as it obeys the relation in 3.18.

It is also important to note that solutions below the line $\Omega_h + \Omega_c = -1$ in figure 3.2 would violate the WEC due to $\Omega_\rho < 0$, and thus should be discarded from further consideration. Red curves on the right represent the closed universe solutions that appear irrelevant to the analysis because trajectories simply diverge as $t \to \infty$.

3.2.2.2 Stabilized fifth dimension and vanishing curvature

Moving beyond the $-1 \leq \omega, \omega_5 \leq 1$ plane, trajectories may be attracted towards the solution $(\Omega_c, \Omega_h) = (0,0)$ for combinations that obey $1 + 2\omega_5 - 3\omega = 0$ and $\omega < -1/3$ simultaneously.

The right panel of figure 3.2 demonstrates how the solution curves behave for the sample set of $\omega = -1$ and $\omega_5 = -2$. Trajectories in both open and closed universe models here emerge from the $(\Omega_c, \Omega_h) = (0,-1)$ state, where the fifth dimension contracts at a rate given by $|h| = H$ in an almost flat universe. For $k = -1$, solutions converge only within the triangular region where they move towards $(\Omega_c, \Omega_h) = (0,0)$. Same behavior applies for any set of EoS parameters in the above category and the only constraint on the states appears to be $\Omega_c + \Omega_h \geq 1$, which follows again from WEC with $\Omega_\rho \geq 0$.

In a closed universe, the saddle alters dramatically for small changes in the EoS parameters and initial conditions become important in determining convergent trajectories.

3.2.2.3 Flat universe as an invariant manifold

The phase plane associated with the system in equation 3.17 has an invariant manifold that is congruent with the line $\Omega_c = 0$. Representing spatial curvature in three dimensions, Ω_c may initially appear to be greater or less than zero for closed and open universe models, respectively. In either case, the preferred curvature applies to the entire evolution of the system for the sign of Ω_c is determined solely by the constant k term coming from the FRW-type metric in 3.6. Mathematically speaking,

no solution curve $(\Omega_c(N), \Omega_h(N))$ may intersect with the above defined line of zero curvature unless originated from a state lying on it.

A flat universe model with $\Omega_c = 0$ produces trajectories that evolve within the invariant manifold and the general problem reduces to that of finding an exact expression for $\Omega_h(N)$ using

$$\frac{d\Omega_h}{dN} = (1+\Omega_h)\left[1+2\omega_5-3\omega+(\omega_5-\Omega_h)\right]. \tag{3.19}$$

Defining $m = \omega_5 - 1$ and $n = (1+2\omega_5-3\omega)/(\omega_5-1)$, one may rewrite the autonomous equation as

$$\frac{d\Omega_h}{dN} = m(1+\Omega_h)(n+\Omega_h) \tag{3.20}$$

and obtain at once the exact solution in the form

$$\left|\frac{1+\Omega_h}{n+\Omega_h}\right| = \left(\frac{a}{a_o}\right)^{m(n-1)}. \tag{3.21}$$

Here a_o appears as an integration constant assigning, in the more general case, a physically allowed value to a(t) which is — parallel to the formulation of standard cosmology — considered to be an increasing function of time.

Going back to the definition of Ω_h in 3.15, it is also possible to express the solution in terms of the relation between time dependent scale factors $a(t)$ and $b(t)$ as

$$b(t) = \frac{b_o}{a_o^n}\left(\left[\frac{a(t)}{a_o}\right]^{-(1-\omega_5)} + \left[\frac{a(t)}{a_o}\right]^{1+2\omega_5-3\omega}\right)^{1/(1-\omega_5)} \tag{3.22}$$

for $\Omega_h \in (-1,1)$. Similar to the previous step, b_o appears as another constant of integration subject to physical limits coming from stabilization.

Considering the special case of a fully isotropic fluid with $\omega = \omega_5$, equation 3.22 becomes

$$b(t) = b_o\, a_o\left(\left[\frac{a(t)}{a_o}\right]^{-(1-\omega_5)} + \left[\frac{a(t)}{a_o}\right]^{1-\omega_5}\right)^{1/(1-\omega_5)}. \tag{3.23}$$

As $t \to \infty$, the first term in brackets vanishes and the contribution from the second term yields a function of the form $b(t) \approx b_o a(t)$ under the reasonable condition $\omega_5 < 1$. The asymptotic behavior of $b(t)$, contrary to the initial contraction implied by equation 3.23, points at an epoch where both scale factors expand at identical rates violating the conditions required for stabilization.

On the other hand, imposing the exact stabilization relation on equation 3.22, one obtains the solution

$$b(t) = b_o\, a_o \left(\left[\frac{a(t)}{a_o} \right]^{-(1-\omega_5)} + 1 \right)^{1/(1-\omega_5)} \tag{3.24}$$

which, straightforwardly leads to the asymptotic behavior

$$\lim_{t\to\infty} b(t) = b_o\,. \tag{3.25}$$

The above result agrees with particular solutions discussed in [35, 37] for static extra dimensions. For the inverse limiting case, equation 3.24 yields

$$\lim_{t\to 0} b(t) = 1/a\,, \tag{3.26}$$

as does the solutions of type $1/a^q$ in [35] for $q = 1$.

Trajectories on the invariant manifold appear in the form of straight lines, directions of which are determined by the stability characteristics of the two fixed points, -1 and $-n$, obtained directly from equation 3.21. Green lines in left and middle panels of figure 3.2 correspond to sample paths in a fully isotropic universe. They are seen to emerge from the state $\Omega_h = -1$ and reach $\Omega_h = +1$ in the long time limit. Clearly, one dimensional system defined for an exactly flat universe cannot achieve stabilization with a fully isotropic fluid, and nor may it do so with a highly relativistic one. Under the constraint $1 + 2\omega_5 - 3\omega = 0$, the green lines in the right panel of figure 3.2 now move towards $\Omega_h = 0$ and trajectories exhibit the same behavior as long as $\omega, \omega_5 > 1$. Namely, in a flat universe, stabilization may only be reached for EoS parameters smaller than one, obeying the relation above.

Table 3.2 : Cosmologically interesting cases listed together with the stability characters of points A,B,C and D at the corresponding locations on the ω, ω_5 plane. The stability properties written in bold are labeled forbidden for they allow $\Omega_h \geq 0$.

	Quadrant	Point A	Point B	Point C	Point D
Isotropic Universe ($\omega = \omega_5$)	1^{st}	Unstable node	Stable node	**Saddle node**	Saddle node
	3^{rd}		Saddle node		**Stable node**
			None	**Stable node**	None
					Saddle node ($\Omega_c \geq 0$)
Stabilization of Extra Dimension ($1+2\omega_5-3\omega=0$)	1^{st} 4^{th} 3^{rd}	Unstable node	Stable node	Saddle node	Saddle node
	3^{rd}[3]		Saddle node	Stable node	None
			None	Stable node	**Saddle node** ($\Omega_c \geq 0$)
Highly-Relativistic Fluid ($\omega_5+3\omega=1$)	1^{st}	Unstable node	Stable node	Saddle node	Saddle node
	4^{th}	Saddle node		Unstable node	

[3]Outside the zone $-1 \leq \omega, \omega_5 \leq 1$ for $\omega < -1/3$ and $\omega_5 < -1$

4. CONCLUSIONS AND FUTURE PROSPECTS

In this work we have tested the viability of a five dimensional cosmological model via dynamical analysis of the autonomous system in 3.17. Assuming a higher dimensional arrangement and following the time-evolution of the appropriate variables, we have sought the possibility of finding attractors that would imply the existence of stable solutions to our problem.

The three meaningful results discussed thoroughly in the previous section bring along certain complications like non-zero spatial curvature, or negative equation of state parameters subject to $\omega_5 < -1$ that contradicts the WEC applied to FRW metric. More precisely, the first case of highly isotropic fluid reaches stable equilibrium where the fifth dimension eventually becomes stabilized. The problem here is that due to the term $\Omega_c = -1$, one either has to turn to pre-inflationary epoch — for which there exits no source of information — or, an additional mechanism is required to recover the flat universe as it is today. The fully isotropic case, subject to same type of evolution, also makes it harder to obtain the three dimensional radiation that is known to obey $p_r = \rho_r/3$. Finally, the conditions required for exact stabilization and flatness together points at some exotic fluid that is anisotropic and for which the EoS parameters are, or at least, one is, outside the conventional interval $\omega_i > -1$.

In search of the yet unknown source that is responsible for the late time acceleration, cosmologists have been proposing various models over the last decade and dynamical systems theory seems to offer a very practical approach for testing the global behavior of cosmological variables in those set-ups. As for the specific category of higher dimensional cosmology, acceleration through dynamical reduction, or as well, the possible nature of dark matter through compactification may be tested in a $1+3+n$ or $1+m+n$ set-up and again, making use of dynamical systems theory one may test whether such universe can evolve to an effective $1+3$ dimensional one.

REFERENCES

[1] **Ade, P. A. R. et al.** (2016). [Planck Collaboration], Planck 2015 results. XIII. Cosmological parameters, *Astron. and Astrophysics*, *594*, astro-ph/1502.01589.

[2] **Hubble, E.** (1929). A Relation between Distance and Radial Velocity among Extra-Galactic Nebulae, *Proceedings of the National Academy of Sciences*, *15*, 168–173.

[3] **Kirshner, R.P.** (2004). Hubble's diagram and cosmic expansion, *Proceedings of the National Academy of Sciences*, *101*, 8–13.

[4] **Riess, A. G. et al.** (1998). [Supernova Search Team Collaboration], Observational Evidence from Supernovae for an Accelerating Universe and a Cosmological Constant, *The Astronomical Journal*, *116*, 1009, astro-ph/9805201.

[5] **Tonry, J. L. et al.** (2003). [Supernova Search Team Collaboration], Cosmological Results from High-z Supernovae, *The Astrophysical Journal*, *594*, 1, astro-ph/0305008.

[6] **Knop, R. A. et al.** (2003). [The Supernova Cosmology Project], New Constraints on Ω_M, Ω_Λ, and w from an Independent Set of 11 High-Redshift Supernovae Observed with the Hubble Space Telescope, *The Astrophysical Journal*, *598*, 102, astro-ph/0309368.

[7] **Riess, A.G. et al.** (2004). [Supernova Search Team Collaboration], Type Ia Supernova Discoveries at $z > 1$ from the Hubble Space Telescope: Evidence for Past Deceleration and Constraints on Dark Energy Evolution, *The Astrophysical Journal*, *607*, 665, astro-ph/0402512.

[8] **Wood-Vasey, W. M. et al.** (2007). [ESSENCE Collaboration], Observational Constraints on the Nature of Dark Energy: First Cosmological Results from the ESSENCE Supernova Survey, *The Astrophysical Journal*, *666*, 694, astro-ph/0701041.

[9] **Dodelson, S.** (2003). *Modern cosmology*, Academic Press, San Diego, CA.

[10] **Cole, Shaun et al.** (2005). [The 2dFGRS Collaboration], The 2dF Galaxy Redshift Survey: power-spectrum analysis of the final data set and cosmological implications, *Monthly Notices of the Royal Astronomical Society*, *362*, 505–534, astro-ph/0501174.

[11] **Heath Jones, D. et al.** (2009). [The 6dFGS Collaboration], The 6dF Galaxy Survey: final redshift release (DR3) and southern large-scale structures,

Monthly Notices of the Royal Astronomical Society, *399*, 683–698, astro-ph/0903.5451.

[12] **Ahn, C.P. et al.** (2014). [SDSS Collaboration], The Tenth Data Release of the Sloan Digital Sky Survey: First Spectroscopic Data from the SDSS-III Apache Point Observatory Galactic Evolution Experiment, *The Astrophysical Journal Supplement Series*, *211*, 17, astro-ph/1307.7735.

[13] **Bennett, C. L. et al.** (2013). [WMAP Collaboration], Nine-year Wilkinson Microwave Anisotropy Probe (WMAP) Observations: Final Maps and Results, *The Astrophysical Journal Supplement Series*, *208*, 20, astro-ph/1212.5225.

[14] **Hinshaw, G. et al.** (2013). [WMAP Collaboration], Nine-year Wilkinson Microwave Anisotropy Probe (WMAP) Observations: Cosmological Parameter Results, *The Astrophysical Journal Supplement Series*, *208*, 19, astro-ph/1212.5226.

[15] **Fixsen, D.J.** (2009). The Temperature of the Cosmic Microwave Background, *The Astrophysical Journal*, *707*(2), 916, astro-ph/0911.1955.

[16] **Tkachev, I.** (2017). Cosmology and Dark Matter, *CERN Yellow Reports: School Proceedings*, *5*, 259, gr-qc/1802.02414.

[17] **Wald, R.M.** (1984). *General relativity*, Chicago Univ. Press, Chicago, IL.

[18] **Weinberg, S.** (1972). *Gravitation and Cosmology: Principles and Applications of the General Theory of Relativity*, Wiley, New York.

[19] **Calcagni, G.** (2017). *Classical and Quantum Cosmology*, Springer International Publishing, Switzerland.

[20] **Perlmutter, S. et al.** (1999). Measurements of Omega and Lambda from 42 High-Redshift Supernovae, *Astrophys. J.*, *517*, 565–586, astro-ph/9812133.

[21] **Copeland, E.J.**, **Sami, M. and Tsujikawa, S.** (2006). Dynamics of Dark Energy, *International Journal of Modern Physics D*, *15*, 1753–1935, hep-th/0603057.

[22] **Baumann, D.** (2009). TASI Lectures on Inflation, hep-th/0907.5424.

[23] **Guth, A.H.** (1981). Inflationary universe: A possible solution to the horizon and flatness problems, *Phys. Rev. D*, *23*, 347–356.

[24] **Linde, A.D.** (1982). A new inflationary universe scenario: A possible solution of the horizon, flatness, homogeneity, isotropy and primordial monopole problems, *Physics Letters B*, *108*, 389–393.

[25] **Albrecht, A. and Steinhardt, P.J.** (1982). Cosmology for Grand Unified Theories with Radiatively Induced Symmetry Breaking, *Phys. Rev. Lett.*, *48*, 1220–1223.

[26] **Wiggins, S.** (1990). *Introduction to Applied Nonlinear Dynamical Systems and Chaos*, Springer-Verlag New York, New York.

[27] **Perko, L.** (2001). *Differential Equations and Dynamical Systems*, Springer-Verlag New York, New York.

[28] **Guckenheimer, J. and Holmes, P.** (1983). *Nonlinear Oscillations, Dynamical Systems, and Bifurcations of Vector Fields*, Springer-Verlag New York, New York.

[29] **Böhmer, C.G. and Chan, N.**, (2016). Dynamical Systems in Cosmology, World Scientific (EUROPE), pp.121–156.

[30] **Bahamonde, S.**, **Boehmer, C.G.**, **Carloni, S.**, **Copeland, E.J.**, **Fang, W. and Tamanini, N.** (2017). Dynamical systems applied to cosmology: dark energy and modified gravity, gr-qc/1712.03107.

[31] **Overduin, J. and Wesson, P.** (1997). Kaluza-Klein gravity, *Physics Reports*, *283*, 303–380.

[32] **Kaluza, T.** (1921). On the Problem of Unity in Physics, *Sitzungsber. Preuss. Akad. Wiss. Berlin (Math. Phys.)*, *1921*, 966–972.

[33] **Klein, O.** (1926). Quantentheorie und fünfdimensionale Relativitätstheorie, *Zeitschrift für Physik*, *37*(12), 895–906.

[34] **Sahdev, D.** (1984). Perfect-fluid higher-dimensional cosmologies, *Phys. Rev. D*, *30*, 2495–2507.

[35] **Mohammedi, N.** (2002). Dynamical compactification, standard cosmology, and the accelerating universe, *Phys. Rev. D*, *65*, 104018, hep-th/0202119.

[36] **Pahwa, I.**, **Choudhury, D. and Seshadri, T.R.** (2011). Late-time acceleration in higher dimensional cosmology, *Journal of Cosmology and Astroparticle Physics*, *9*, 015, gr-qc/1104.1925.

[37] **Bringmann, T.**, **Eriksson, M. and Gustafsson, M.** (2003). Cosmological evolution of homogeneous universal extra dimensions, *Physical Review D*, *68*(6), 063516, astro-ph/0303497.

[38] **Bringmann, T. and Eriksson, M.** (2003). Can homogeneous extra dimensions be stabilized during matter domination?, *Journal of Cosmology and Astroparticle Physics*, *10*, 006, astro-ph/0308498.

[39] **Gu, J.A. and Hwang, W.Y.P.** (2002). Accelerating universe from the evolution of extra dimensions, *Phys. Rev. D*, *66*, 024003, astro-ph/0112565.

[40] **Gu, J.A.**, (2011). A way to the dark side of the universe through extra dimensions, World Scientific, pp.124–133, astro-ph/0209223.

[41] **Darabi, F.** (2003). An accelerating universe and dynamical compactification of extra dimensions, *Classical and Quantum Gravity*, *20*, 3385, gr-qc/0301075.

[42] **Georgalas, B.C.**, **Karydas, S. and Papantonopoulos, E.** (2017). Reconstruction of Cosmological Evolution in the Presence of Extra Dimensions, gr-qc/1711.02723.

[43] **Deffayet, C.**, **Dvali, G. and Gabadadze, G.** (2002). Accelerated universe from gravity leaking to extra dimensions, *Phys. Rev. D*, *65*, 044023, astro-ph/0105068.

[44] **Sahni, V. and Shtanov, Y.** (2003). Braneworld models of dark energy, *Journal of Cosmology and Astroparticle Physics*, *2003*(11), 014, astro-ph/0202346.

[45] **Maia, M.**, **Monte, E.M. and Maia, J.** (2004). The accelerating universe in brane-world cosmology, *Physics Letters B*, *585*(1), 11 – 16, astro-ph/0208223.

[46] **Perivolaropoulos, L. and Sourdis, C.** (2002). Cosmological effects of radion oscillations, *Phys. Rev. D*, *66*, 084018, hep-ph/0204155.

[47] **Brax, P.**, **van de Bruck, C.**, **Davis, A.C. and Rhodes, C.S.** (2003). Cosmological evolution of brane world moduli, *Phys. Rev. D*, *67*, 023512, hep-th/0209158.

[48] **Brax, P.**, **van de Bruck, C.**, **Davis, A.C. and Rhodes, C.** (2003). Varying Constants in Brane World Scenarios, *Astrophysics and Space Science*, *283*(4), 627–632, hep-ph/0210057.

[49] **Binétruy, P.**, **Deffayet, C. and Langlois, D.** (2001). The radion in brane cosmology, *Nuclear Physics B*, *615*(1), 219 – 236, hep-th/0101234.

[50] **Randall, L. and Sundrum, R.** (1999). An Alternative to Compactification, *Physical Review Letters*, *83*, 4690–4693, hep-th/9906064.

[51] **Randall, L. and Sundrum, R.** (1999). Large Mass Hierarchy from a Small Extra Dimension, *Physical Review Letters*, *83*, 3370–3373, hep-ph/9905221.

[52] **Arkani-Hamed, N.**, **Dimopoulos, S. and Dvali, G.** (1998). The hierarchy problem and new dimensions at a millimeter, *Physics Letters B*, *429*, 263–272, hep-ph/9803315.

[53] **Dvali, G.**, **Gabadadze, G. and Porrati, M.** (2000). 4D gravity on a brane in 5D Minkowski space, *Physics Letters B*, *485*, 208–214, hep-th/0005016.

[54] **Maartens, R.** (2004). Brane-World Gravity, *Living Reviews in Relativity*, *7*, 7, gr-qc/0312059.

[55] **Appelquist, T. and Dobrescu, B.A.** (2001). Universal extra dimensions and the muon magnetic moment, *Physics Letters B*, *516*, 85–91, hep-ph/0106140.

[56] **Townsend, P.K. and Wohlfarth, M.N.** (2003). Accelerating Cosmologies from Compactification, *Physical Review Letters*, *91*(6), 061302, hep-th/0303097.

[57] **Cline, J.M. and Vinet, J.** (2003). Problems with time-varying extra dimensions or "Cardassian expansion" as alternatives to dark energy, *Phys. Rev. D*, *68*, 025015, hep-ph/0211284.

[58] **Uzan, J.P.** (2003). The fundamental constants and their variation: observational and theoretical status, *Rev. Mod. Phys.*, *75*, 403–455, hep-ph/0205340.

APPENDICES

APPENDIX A.1 : Field Equations in Five Dimensions
APPENDIX A.2 : Continuity Equation of the Higher Dimensional Fluid
APPENDIX A.3 : Autonomous Equations

APPENDIX A.1

$$g_{AB} = \begin{pmatrix} -1 & & & & \\ & \frac{a^2(t)}{1-kr^2} & & & \\ & & a^2(t)r^2 & & \\ & & & a^2(t)r^2 sin^2\theta & \\ & & & & b^2(t) \end{pmatrix} \tag{A.1}$$

Non-zero Christoffel Symbols:

$$\begin{aligned} \Gamma^0{}_{ij} &= \frac{\dot{a}}{a} g_{ij}, & \Gamma^0{}_{55} &= \frac{\dot{b}}{b} g_{55} \\ \Gamma^i{}_{j0} &= \Gamma^i{}_{0j} = \delta^i_j \frac{\dot{a}}{a}, & \Gamma^5{}_{50} &= \Gamma^5{}_{05} = \frac{\dot{b}}{b} \\ \Gamma^1{}_{11} &= \frac{kr}{1-kr^2}, & \Gamma^1{}_{22} &= r(kr^2-1), & \Gamma^1{}_{33} &= rsin^2\theta(kr^2-1) \\ \Gamma^2{}_{12} &= \Gamma^2{}_{21} = \frac{1}{r}, & \Gamma^2{}_{33} &= -\sin\theta\cos\theta \\ \Gamma^3{}_{13} &= \Gamma^3{}_{31} = \frac{1}{r}, & \Gamma^3{}_{23} &= \Gamma^3{}_{32} = \cot\theta \end{aligned} \tag{A.2}$$

Diagonal elements of the Riemann tensor for $A,B,C = 0,1,2,3,5$ and $i,j = 1,2,3$:

$$\begin{aligned} R_{AB} =& (\Gamma^C{}_{AB})_{,C} - (\Gamma^C{}_{AC})_{,B} + \Gamma^C{}_{AB}\Gamma^D{}_{CD} - \Gamma^C{}_{AD}\Gamma^D{}_{BC} \\ R_{00} =& -\left[(\Gamma^i{}_{0i})_{,0} + (\Gamma^5{}_{05})_{,0}\right] - \Gamma^i{}_{0j}\Gamma^j{}_{0i} - \Gamma^5{}_{05}\Gamma^5{}_{05} \\ =& -\{3\frac{\ddot{a}}{a} + \frac{\ddot{b}}{b}\} \end{aligned} \tag{A.3}$$

$$\begin{aligned} R_{11} = (\Gamma^0{}_{11})_{,0} + (\Gamma^1{}_{11})_{,1} - (\Gamma^i{}_{1i})_{,1} + \Gamma^0{}_{11}(\Gamma^i{}_{0i} + \Gamma^5{}_{05}) + \Gamma^1{}_{11}\Gamma^i{}_{1i} - 2\Gamma^0{}_{11}\Gamma^1{}_{10} \\ - \Gamma^i{}_{1j}\Gamma^j{}_{1i} \\ = \frac{a^2}{1-kr^2}\{\frac{\ddot{a}}{a} + 2\frac{\dot{a}^2}{a^2} + \frac{\dot{a}}{a}\frac{\dot{b}}{b} + \frac{2k}{a^2}\} \end{aligned} \tag{A.4}$$

$$\begin{aligned} R_{22} = (\Gamma^0{}_{22})_{,0} + (\Gamma^1{}_{22})_{,1} - (\Gamma^3{}_{23})_{,2} + \Gamma^0{}_{22}(\Gamma^i{}_{0i} + \Gamma^5{}_{05}) + \Gamma^1{}_{22}\Gamma^i{}_{1i} - 2\Gamma^0{}_{22}\Gamma^2{}_{20} \\ - 2\Gamma^1{}_{22}\Gamma^2{}_{21} - \Gamma^3{}_{23}\Gamma^3{}_{23} \\ = a^2r^2\{\frac{\ddot{a}}{a} + 2\frac{\dot{a}^2}{a^2} + \frac{\dot{a}}{a}\frac{\dot{b}}{b} + \frac{2k}{a^2}\} \end{aligned} \tag{A.5}$$

Similarly,

$$R_{33} = a^2r^2sin^2\theta\{\frac{\ddot{a}}{a} + 2\frac{\dot{a}^2}{a^2} + \frac{\dot{a}}{a}\frac{\dot{b}}{b} + \frac{2k}{a^2}\} \tag{A.6}$$

$$\begin{aligned} R_{55} =& (\Gamma^0{}_{55})_{,0} + \Gamma^0{}_{55}(\Gamma^i{}_{0i} + \Gamma^5{}_{05}) - 2\Gamma^5{}_{05}\Gamma^0{}_{55} \\ =& b^2\{\frac{\ddot{b}}{b} + 3\frac{\dot{b}}{b}\frac{\dot{a}}{a}\} \end{aligned} \tag{A.7}$$

Ricci Scalar:

$$R = g^{AB}R_{AB} = g^{00}R_{00} + g^{11}R_{11} + g^{22}R_{22} + g^{33}R_{33} + g^{55}R_{55}$$

$$R = 6\frac{\ddot{a}}{a} + 2\frac{\ddot{b}}{b} + 6\left(\frac{\dot{a}}{a}\right)^2 + 6\frac{\dot{a}}{a}\frac{\dot{b}}{b} + 6\frac{k}{a^2} \tag{A.8}$$

Non-zero elements of the Einstein tensor:

$$G_{AB} = R_{AB} - \frac{1}{2}Rg_{AB}$$

$$G_{00} = 3\left(\frac{\dot{a}}{a}\right)^2 + 3\frac{\dot{a}}{a}\frac{\dot{b}}{b} + 3\frac{k}{a^2} \tag{A.9}$$

$$\begin{aligned} G_{11} &= \frac{a^2}{(1-kr^2)}\{-2\frac{\ddot{a}}{a} - \left(\frac{\dot{a}}{a}\right)^2 - 2\frac{\dot{a}}{a}\frac{\dot{b}}{b} - \frac{\ddot{b}}{b} - \frac{k}{a^2}\} \\ G_{22} &= a^2r^2\{-2\frac{\ddot{a}}{a} - \left(\frac{\dot{a}}{a}\right)^2 - 2\frac{\dot{a}}{a}\frac{\dot{b}}{b} - \frac{\ddot{b}}{b} - \frac{k}{a^2}\} \\ G_{33} &= a^2r^2sin^2\theta\{-2\frac{\ddot{a}}{a} - \left(\frac{\dot{a}}{a}\right)^2 - 2\frac{\dot{a}}{a}\frac{\dot{b}}{b} - \frac{\ddot{b}}{b} - \frac{k}{a^2}\} \end{aligned} \tag{A.10}$$

and

$$G_{55} = b^2\{-3\frac{\ddot{a}}{a} - 3\left(\frac{\dot{a}}{a}\right)^2 - 3\frac{k}{a^2}\} \tag{A.11}$$

For $g_{AC}T^C{}_B = T_{AB}$ and $G_{AB} = \kappa_5 T_{AB}$, five dimensional field equations are:

$$\begin{aligned} 3\left(\frac{\dot{a}}{a}\right)^2 + 3\frac{\dot{a}}{a}\frac{\dot{b}}{b} + 3\frac{k}{a^2} &= \kappa_5\rho \\ -2\frac{\ddot{a}}{a} - \left(\frac{\dot{a}}{a}\right)^2 - 2\frac{\dot{a}}{a}\frac{\dot{b}}{b} - \frac{\ddot{b}}{b} - \frac{k}{a^2} &= \kappa_5 p \\ -3\frac{\ddot{a}}{a} - 3\left(\frac{\dot{a}}{a}\right)^2 - 3\frac{k}{a^2} &= \kappa_5 p' \end{aligned} \tag{A.12}$$

APPENDIX A.2

Defining $\frac{\dot{a}}{a} = H$ and $\frac{\dot{b}}{b} = h$, and also, $p = \omega\rho$ and $p' = \omega_5\rho$, field equations may be rearranged as

$$3H^2 + 3Hh + 3\frac{k}{a^2} = \kappa_5\rho \tag{A.13}$$

$$-2\dot{H} - 3H^2 - 2Hh - \dot{h} - h^2 + \frac{k}{a^2} = \kappa_5(\omega\rho) \tag{A.14}$$

$$-3\dot{H} - 6H^2 - 3\frac{k}{a^2} = \kappa_5(\omega_5\rho) \tag{A.15}$$

Differentiating **A.13** wrt t,

$$6H\dot{H} + 3\dot{H}h + 3H\dot{h} - 6H\frac{k}{a^2} = \kappa_5\dot{\rho} \tag{A.16}$$

multiplying **A.14** with $3H$,

$$-6\dot{H}H - 9H^3 - 6H^2h - 3H\dot{h} - 3Hh^2 - 3H\frac{k}{a^2} = 3H\kappa_5(\omega\rho) \tag{A.17}$$

again, **A.13** with $3H$,

$$9H^3 + 9H^2h + 9H\frac{k}{a^2} = 3H\kappa_5\rho \tag{A.18}$$

now with h,

$$3H^2h + 3Hh^2 - 3h\frac{k}{a^2} = h\kappa_5\rho \tag{A.19}$$

and finally, **A.15** with h,

$$-3\dot{H}h - 6H^2h - 3h\frac{k}{a^2} = h\kappa_5(\omega'\rho) \tag{A.20}$$

one obtains the continuity equation through the addition of **A.16**-**A.20**:

$$\boxed{\dot{\rho} + 3H(\rho + \omega\rho) + h(\rho + \omega_5\rho) = 0} \tag{A.21}$$

APPENDIX A.3

$$1 + \underbrace{\frac{h}{H}}_{\Omega_h} + \underbrace{\frac{k}{a^2H^2}}_{\Omega_c} = \underbrace{\frac{\kappa_5\rho}{3H^2}}_{\Omega_\rho} \tag{A.22}$$

$$\frac{d}{dt}\Omega_c = -k(\frac{2\dot{a}}{a^3H^2} + \frac{2\dot{H}}{a^2H^3}) = -2H\Omega_c - 2\Omega_c\frac{\dot{H}}{H}$$

From **A.15**,

$$\frac{\dot{H}}{H^2} = -\left[\frac{\kappa_5(\omega_5\rho)}{3H^2} + \frac{k}{a^2H^2} + 2\right] \tag{A.23}$$

$$\frac{1}{H}\frac{d}{dt}\Omega_c = \Omega_c' = -2\Omega_c - 2\Omega_c\left[-2 - \Omega_c - \omega_5(1 + \Omega_h + \Omega_c)\right]$$

$$\boxed{\Omega_c' = 2\Omega_c\left[\Omega_c + \omega_5(1 + \Omega_h + \Omega_c) + 1\right]} \tag{A.24}$$

$$\frac{d}{dt}\Omega_h = \frac{\dot{h}}{H} - \frac{\dot{H}}{H}\frac{h}{H} = \frac{\dot{h}}{H} - \frac{\dot{H}}{H}\Omega_h$$

$$\Omega_h' = \frac{\dot{h}}{H^2} - \frac{\dot{H}}{H^2}\Omega_h$$

From **A.14**,

$$\frac{\dot{h}}{H^2} = -\left[2\frac{\dot{H}}{H^2} + 3 + 2\frac{h}{H} + \left(\frac{h}{H}\right)^2 + \frac{k}{a^2H^2} + 3\omega\frac{\kappa_5\rho}{3H^2}\right] \tag{A.25}$$

$$\Omega_h' = -2\frac{\dot{H}}{H^2} - 3 - 2\Omega_h - \Omega_h^2 - \Omega_c - 3\omega(1+\Omega_h+\Omega_c) - \frac{\dot{H}}{H^2}\Omega_h$$

$$= -2\left[-2-\Omega_c-\omega_5(1+\Omega_h+\Omega_c)\right] - 3 - 2\Omega_h - \Omega_h^2 - \Omega_c - 3\omega(1+\Omega_h+\Omega_c) \\ -\Omega_h\left[-2-\Omega_c-\omega_5(1+\Omega_h+\Omega_c)\right]$$

$$\boxed{\Omega_h' = 1-\Omega_h^2+\Omega_c(1+\Omega_h)+(1+\Omega_c+\Omega_h)\left[(2+\Omega_h)\omega_5-3\omega\right]} \qquad \textbf{(A.26)}$$

CURRICULUM VITAE

Name Surname: Ezgi Canay

Place and Date of Birth: Istanbul, 08/10/1989

E-Mail: ezgicanay@itu.edu.tr

EDUCATION:

- **B.Sc.:** 2013, Istanbul Technical University, Faculty of Science and Letters, Department of Engineering Physics

PROFESSIONAL EXPERIENCE AND REWARDS:

- 05/2017- Research Assistant at Istanbul Technical University, Department of Engineering Physics
- 09/2013-04/2014 Teaching Assistant at Sabancı University

PUBLICATIONS, PRESENTATIONS AND PATENTS ON THE THESIS:

- Arapoğlu, A.S., Canay, E., Yükselci, A.E., 2018. Dynamical System Analysis of a Five-Dimensional Cosmological Model, gr-qc/1801.08402